OTC 14OTC-P-1506-OTC

Carbon Nanotube Composite Cables for Ultra-Deepwater Oil and Gas Fields

T. G. Holesinger, R. DePaula, and John Rowley, Los Alamos National Laboratory; K. Sperling, SPE, Chevron; J. M. Pappas, SPE, Research Partnership to Secure Energy for America

This paper was prepared for presentation at the Offshore Technology Conference held in Houston, Texas, USA, 5–8 May 2014.

Abstract

This work summarizes our progress on the development of carbon nanotube (CNT) composite cables for ultra-deepwater oil and gas fields. Near- and long-term intended applications include, for example, more efficient hangar penetrations, sub-sea floor power distribution, and ultra-deepwater dynamic power umbilicals. The project goals are to produce by scalable production methods high-conductivity CNT composite wires that can be wound together to make under sea (and / or in-wellbore) cables. In order to the make practical use of the nanotubes, technologies need to be developed that can deal with or manipulate CNTs in great quantities. For power transmission applications one will need to make dense structures of the CNTs that are aligned simultaneously along the direction of current flow. Also, methodologies that can electrically connect the tubes together in their transverse direction are needed to enable high percolation conductivity though the entire CNT/Metal matrix ensemble. In this work we will summarize our progress towards CNT wire development with descriptions of the wire processing, wire performance, and correlation of performance with structural properties. To date, we have successfully produced wires that display high conductivity values for CNT coatings. Addtionally, these conductors are much lighter compared to pure Cu wires and offer additional advantages for applications needing lightweight materials. Prospects for near and long-term application testing will be discussed.

Introduction

Ever since their discovery in 1991 by Iijima (Iijima 1991), carbon nanotube (CNT) conductors have intrigued scientists and engineers with their spectacular properties with respect to electrical conductivity, strength, and thermal conductivity(De Volder et al. 2013). Many efforts are underway to assemble CNTs into components for use in large-scale applications. With respect to electrical conductivity, many research programs are in place to develop CNT-based conductors and cables for use in the microelectronics, electric utility, medical, aerospace, and transportation industries. Many of the strategies employed for producing these conductors have focused on the development of CNT fibers with reported resistivities spanning several orders of magnitude above that of oxygen free copper (1.68 μΩ-cm) (Behabtu et al. 2013, Zhao et al. 2011, Liu et al. 2010, Miao 2011, Li and Chou 2009). Of note are the recent works using chlrosulfonic acid based solutions for CNT fiber extrusion and iodine-doped CNT cables where resistivity levels were found to be just one order of magnitude higher than copper (Cu) with the specific conductivity of these cables (conductivity/weight), exceeding that for all metals except sodium (Behabtu et al. 2013) (Zhao et al. 2011).

In the oil and gas industry, ever increasing power needs for deep-water exploration has led to the need to develop conductors that are better than copper and able to transmit more power to the sub-sea floor. Near-term opportunities include improving or enabling downhole electrical submersible pumps, operation at lower voltages to improve reliability, and increasing electrical transmissibility through the available wellhead space. Longer term opportunities exist for the development of ultra-deepwater dynamic umbilicals that have superior mechanical performance compared to existing technologies, make more efficient use of the existing footprint at the well site, enable higher power transmission efficiency leading to longer tieback distances, and reduce the power transmission voltage for addressing safety, topside space, and reliability issues. We

discuss here our first results and progress to develop a CNT composite conductor that addresses these issues, with the ultimate goal of producing conductor that has conductivity greater than that of copper wire. Our approach has been to develop a coating process to align CNTs as a dense, thick film onto a wire former to produce a wire that in the end can be field deployed and handled much like a conventional copper wire or cable. This approach also is the results in a conductor which is significantly lighter than Cu, offering advantages in applications where light weighting is also needed.

Discussion

Experimental.

The CNT copper composite wires were prepared by dip-coating CNT solutions onto a copper wire former, which for these initial studies was a 20, 26, or 28 AWG wire size (approximately 0.81, 0.45, or 0.31 mm diameter, respectively) Cu wire. Multi-walled (MW)-CNTs were used in the production of the solutions and were obtained from arrays grown using ethylene as the source gas. (Li et al. 2006). The length of the MW-CNTs ranged from 0.5 to 3 mm, depending on the amount of time used to grow the arrays. Because these CNTs were taken from grown arrays, the CNTs used for any one solution were essentially the same length. Additional details of the growth process can be found elsewhere (Li et al. 2006). The solutions were either water-based, prepared with one of the two dispersants Triton-C or Dawn® detergent, or sulfuric acid-based. The water-based solutions were mixed in the ratio of 1.75 to 3.5 ml of dispersant to 10 mg of CNT, typical of what has been reported previously (Rastogi et al. 2008). Solutions consisted of 10 to 20 mg of CNTs in 300 ml of distilled water. Solutions were stirred without ultrasonic agitation to produce CNT solutions consisting of individual and small fibers of CNTs. The deliberate avoidance of ultrasonic agitation minimized CNT damage. Likewise, acid-based solutions of CNT have been reported(Behabtu et al. 2013) and the ones used here consisted of technical-grade sulfuric acid, with the CNTs dispersed in the solution with stirring. In both cases, the CNTs were not completely dissolved into solution as extended fiber structures were present. The copper wire formers were first abraded with 240 grit SiC paper, ultrasonically cleaned in acetone and isopropanol, and then etched for one minute in a dilute HCl acid solution, followed by a final water rinse and air dry. The composite wires were formed by dip-coating the copper wires with the solution, followed by rinsing in isopropanol to remove the water and dispersant, or just water to remove the acid, and then drying on a hot plate at 100ºC. Coated sections of wires were at least 15 cm in length. For some the acid-based samples, conventional wire drawing was also investigated as a means to improve the density and alignment of the CNT coatings on the wires. Additional copper was added in some cases to the CNT coatings through solution deposition of a Cu-salt or sputter coating of Cu metal in order to improve the electrical contact between the CNTs (Holesinger 2013). Wires were heat treated in inert (Ar) or reducing atmosphere (6% H_2/Ar) across a range of temperatures from 300 ºC to 900ºC for some of the samples after the dip-coating and solution deposition steps. Sputter coating was also used in a few cases to deposit approximately 100 nm of Cu on the outside of the wire coating. The 100 nm of Cu was much less than the overall thicknesses of the CNT coatings, which were in the range of 10 to 200 μm. For each wire, a piece of the starting substrate was cut off and kept with the sample. This companion sample did not have any CNT or Cu deposition from the coating processes, but it did accompany the coated wire through any heat treatments. This bare substrate wire was measured to determine a resistivity value for the Cu wire core of each wire.

Samples were primarily characterized by measurement of the electrical resistance of the CNT composite wire and the reference bare substrate wire at room temperature, measurement of the copper wire substrate and CNT composite wire diameters with a laser micrometer (AEROEL XLS13XY Laser Scan Micrometer), and the examination of the conductors by (FEI Inspect) scanning electron microscopy (SEM) and (FEI Tecnai TF-30) (scanning) transmission electron microscope (STEM / TEM). The resistivity values were calculated from the resistance (Keithley 2000 multimeter) across a measured length with test currents of 100, 30, and 10 mA (Lakeshore 120 Current Source). At least 10 measures of the wire diameter were taken over the length measured for resistance and averaged to give the diameter (and coating thickness) of the wire. Most of the SEM work consisted of imaging the wires in their as-processed state. A few wires were prepared for cross-sectional microscopy by conventional mounting and polishing using SiC papers and diamond grits. Samples were cut and mounted for cross-sectional or plan-view imaging. Epoxy was poured around and over the samples placed in a mounting cup. This setup was then evacuated in a small pumping chamber to remove gas from internal pores within the wires. After this step, the samples were pressurized to 1000 psig to force the epoxy into the void space for structural support. After curing, the samples were then polished, etched, and carbon-coated for viewing in the SEM. Additional microstructural analysis of the CNTs used in the conductors was carried out in a FEI Tecnai TF-30.

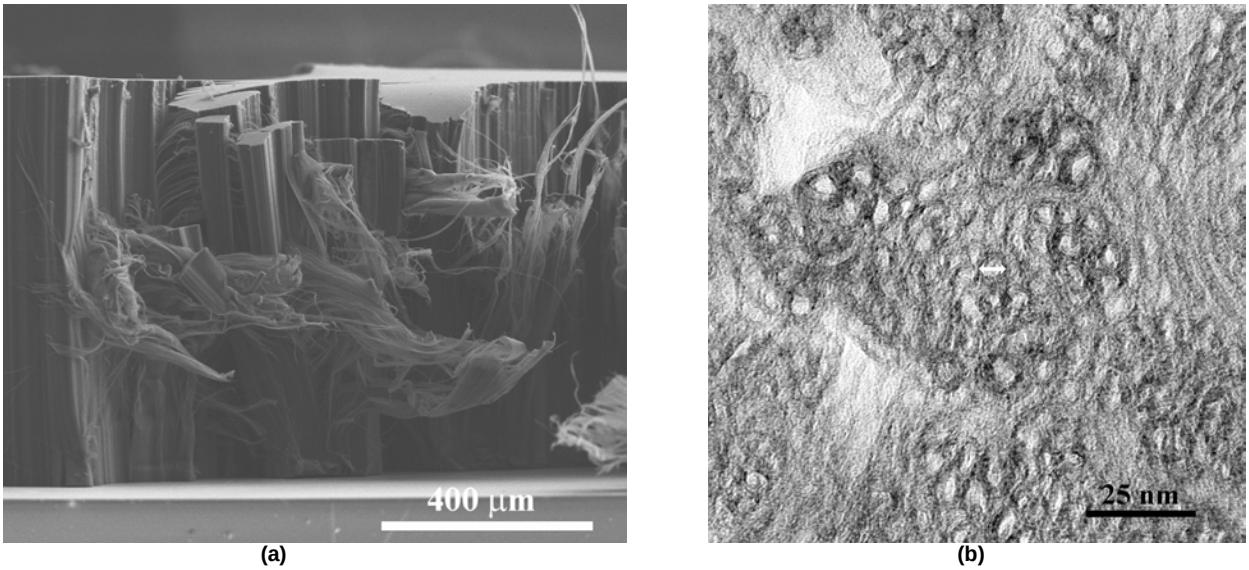

(a) (b)

Figure 1: SEM image (a) of an as-grown, 0.75 mm tall multi-wall CNT array that is the source for the CNT solutions in this work. TEM cross-sectional showing a cross-section of a CNT bundle. The white arrow in the center the cross-section of one CNT. The average diameter on the MW-CNTs was 10 nm.

Results

Carbon Nanotube Arrays.

Shown in Figure 1 are SEM images of a 0.75 mm tall, as-grown array and a TEM image of the multi-wall nanotubes that result from the growth process. This was one of the shorter forests used for the CNTs. Typically, the forests used ranged in height from 1.5 to 2 mm, although forests as tall as 3 mm were used as well. In general, the taller the forest, the more time intensive the solution preparation process became to prepare solutions containing individual CNTs and small extended fibers of CNTs for the coating process. The multi-wall CNTs were on average 10 nm in diameter. As mentioned above, the lengths of the CNTs were very well defined based on the solution process used and the avoidance of ultrasonic assistance in solution development.

Water-Based CNT Composite Conductors.

CNT coatings of various thicknesses were made onto Cu wires with water-based solutions. Shown in Figures 2a and b are SEM images of relatively thin coatings from water-based solutions on the larger 20 AWG Cu wire. The coating is relatively smooth and comprised of extended CNT fibers generally aligned along the axis of the wire. The TEM image of Figure 2c shows that the CNT bundles are tightly packed in these thin coatings. For the thicker coatings, a much rougher surface morphology was found (Figures 2d and e). In cross-section, these thicker coatings were found to have porosity and substantial thickness variations around the wire. For some of the samples processed with added Cu via solution deposition, a fine dispersion of Cu particles (small bright spots) resulted after a subsequent heat treatment of the coated wire (Fig. 2f and g). The sample shown in Figure 2f had a thick gold layer sputtered onto it for protection during the cross-sectional sample preparation process. The copper from the solution deposition did not form a continuous matrix within the CNT coatings as shown in Figure 2g.

Acid-Based CNT Composite Conductors.

Coatings were also made onto Cu wire formers with the sulfuric-acid based solutions. In addition, these wires were drawn with conventional wire dies to gauge the effects of mechanical deformation on CNT alignment and densification. Shown in Figures 3a and b are images of CNT wires in the as-coated and wire-drawn states. The wire drawing clearly helped shape and densify the thick CNT coatings, as well as improve the alignment within the CNT coatings as shown in Fig. 3c. Note that the long axis of the wire is parallel to the bottom of the latter image. Without wire drawing, the CNT coatings were very similar to the composite wires produced from the water-based solutions. For this set of wires, the addition of Cu via solution deposition was not undertaken.

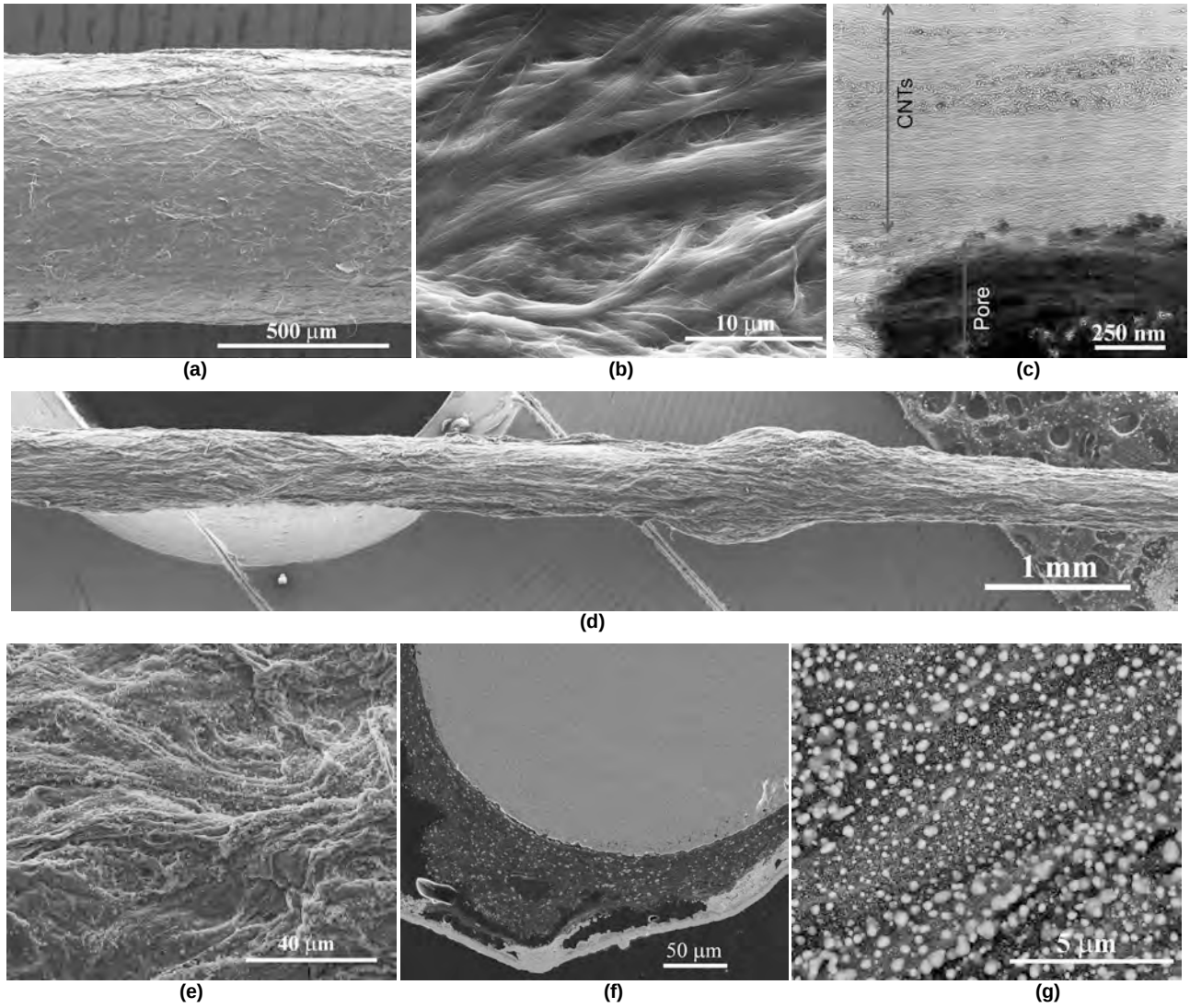

Figure 2: SEM images of CNT coatings made from water-based solutions. Images (a) and (b) are of a thinly coated CNT wire in which the 20 AWG Cu wire served as the wire template. The bright field TEM image (c) is a cross-sectional view of the thin CNT coating on wire. SEM images (d) and (e) show a thick-coat CNT composite wire where the wire former was 28 AWG Cu wire. Image (f) is a cross-sectional SEM image of the thick CNT coating while (g) shows the Cu nanoparticles that are present in samples in which Cu was added by solution deposition. For (a), (b), (e), and (g), the long axis of the wire is parallel to the bottom of the images.

Resistivity Measurements.

Tables 1 and 2 contain the direct measurements of the overall wire resistivities of composite wires produced from water or sulfuric based solutions, respectively. The CNT coating resistivity values were obtained by calculating the parallel resistance value of the coating given the resistivity of the wire substrate (obtained from the bare witness Cu substrate wire), the dimensions of the overall wire and copper wire substrate.

$$\frac{1}{R_{wire}} = \frac{1}{R_{CNT}} + \frac{1}{R_{Cu}}$$

Solving for the resistivity (ρ_{CNT}) of the CNT coating, we obtain:

$$\rho_{CNT} = \frac{(A_{wire}-A_{Cu})*\rho_{Cu}*\rho_{wire}}{A_{wire}*\rho_{Cu}-A_{Cu}*\rho_{wire}}$$

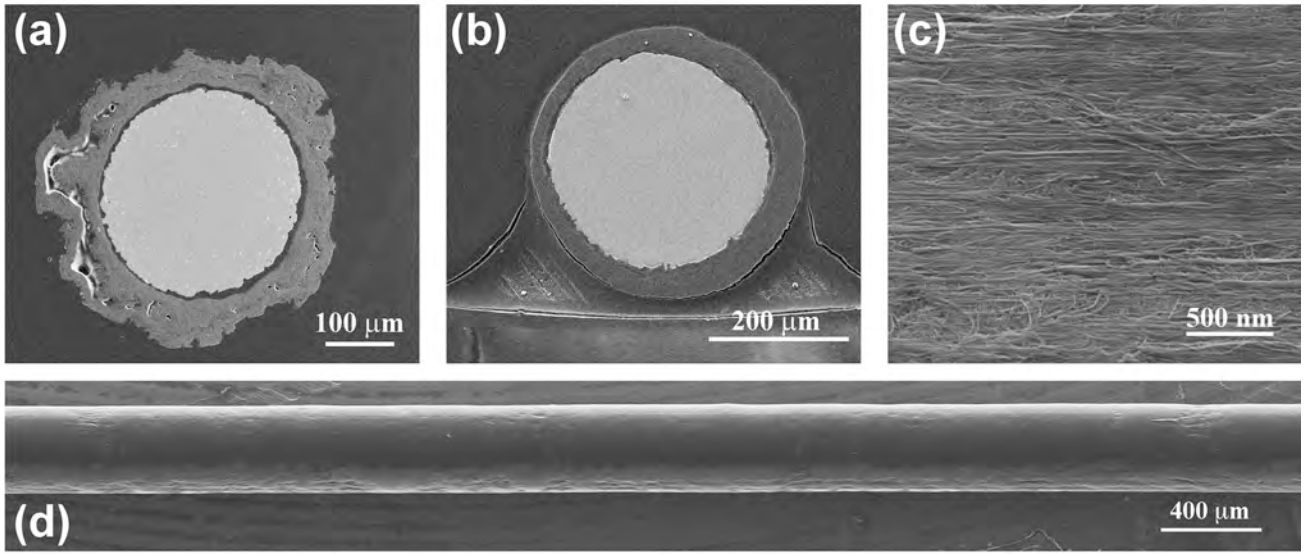

Figure 3: SEM images of CNT coatings made from acid-based solutions. Images (a) and (b) are of a coated CNT wires with the sample in (b) having been wire drawn after coating. The SEM image (c) shows the relatively good CNT alignment within the coating. The long axis of the wire is parallel to the image bottom. The SEM composite image (d) shows an overall uniform surface morphology of a thick CNT coating after the wire drawing steps.

The cross-sectional areas, A_{wire} and A_{Cu}, and resistivities, ρ_{wire} and ρ_{Cu}, refer to the fully-processed coated wires and Cu wire substrates, respectively. The resistivity of the bare Cu substrate that accompanied each coated wire was used for the value of Cu in the calculations and can be found in Table 1.

Shown in Table 1 are measured wire resistivities and calculated CNT coating resistivities of some wires produced from water-based solutions in this work. Also included in Table 1 are wire resistivity values for Cu and Al (Weast 1983). Table 2 contains the data for the CNT wires produced from acid based solutions. For reference, the measurement of the wire used in the experiments is also included. Note that the abrading and etching of the Cu wire prior to CNT coat increases the resistivity of the Cu wire formers. While no wire was better than copper, many of the composite wires with thick CNT coatings had lower resistivity values compared to Al. In a few cases, the calculated resistivity values of the thinnest CNT coatings were approaching those of copper. In most cases, the calculated resistivities of the CNT coatings were more than an order of magnitude higher compared to copper. The fraction of the wire cross-section represented by the CNT coating of these latter samples was greater than 20 percent. Some coatings contained significant structural defects which rendered the coatings non-conductive such as the crack structures shown in Figure 4. This could also be seen in the direct measurement of the resistance over a given length. The addition of an electrically conductive coating resulted in a lower resistance per unit length compared to the bare witness wires. Coatings with significant structural defects were correlated with higher resistances per unit length when compared to their Cu witness samples.

Conclusions and Recommendations

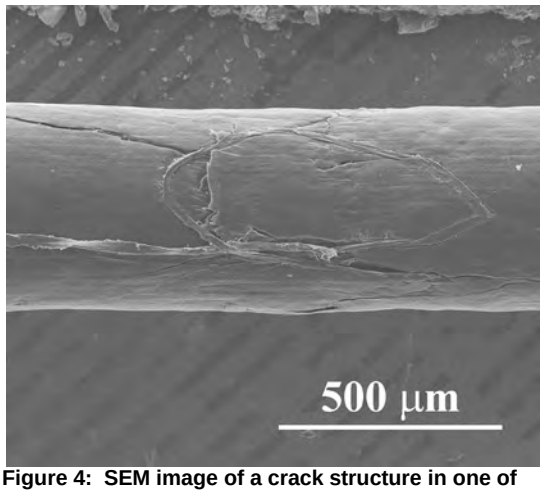

Figure 4: SEM image of a crack structure in one of the CNT coated wires after wire drawing.

We have pursued the coated conductor approach in developing a CNT composite wire with the goal of developing a CNT-based wire that has the characteristics of a conventional wire in terms of its handling and field deployment, yet is much lighter and has resistivity values comparable to those of Cu. This novel approach makes some sacrifices in terms of the specific conductivity (Zhao et al. 2011, Behabtu et al. 2013). These initial results presented here show that significant progress has been made towards producing such a CNT composite wire that can be handled like a conventional copper wire for power applications.

The resistivity values obtained for the composite wires and calculated for the CNT coatings are encouraging when compared to the best reported values for pure CNT fibers in the literature (see (Zhao et al. 2011) and references within). These relatively high values are not due to a connected copper matrix within the CNT matrix that acts as a shunt. As shown in Figure 2g, the copper from the solution deposition process results in a discreet decoration of the CNTs with nanoparticles. The copper was put into the CNT matrix in the water-based samples as a

Table 1: List of CNT coated wire and calculated CNT coating resistivities along with typical resistivity values for copper and aluminum in wire form (Weast 1983).

Wire	Wire Substrate	Dispersant	Wire Resistivity (μΩ-cm)	Substrate Resistivity (μΩ-cm)	Calculated CNT Coating Resistivity (μΩ-cm)	Coating Thickness (μm)	CNT Coating: Percentage of Cross-Section
Cu (O_2 free)	---		1.68	---	---	---	---
Cu (annealed)	---		1.72	---	---	---	---
Cu (hard drawn)	---		1.77	---	---	---	---
Al	---		2.82	---	---	---	---
17_7	20 AWG Cu	water/Dawn	1.88	1.79	4.8	15.6	7.5%
7_7	20 AWG Cu	water/Dawn	1.82	1.77	2.7	19.5	9.4%
24_3	28 AWG Cu	water/Dawn	2.48	1.86	17.3	21.7	23.1%
33_2	28 AWG Cu	water/Triton X	2.52	1.84	37.5	29.2	29.3%
28_1	28 AWG Cu	water/Dawn	2.78	1.87	23.6	43.4	38.7%
16_7	20 AWG Cu	water/Dawn	2.26	1.82	19.0	49.9	21.7%
17_3	20 AWG Cu	water/Dawn	2.3	1.82	41.6	52.1	22.0%
29_2	28 AWG Cu	water/Dawn	3.19	1.85	20.9	53.8	46.2%
32_2	28 AWG Cu	water/Triton X	3.68	1.86	29.9	67.0	52.7%
6_1	20 AWG Cu	water/Dawn	2.53	1.84	22.3	77.4	29.8%
30_2	28 AWG Cu	water/Dawn	4.72	1.77	48.9	105.0	64.9%
30_1	28 AWG Cu	water/Dawn	5.55	1.90	45.0	110.0	66.1%
27_1	28 AWG Cu	water/Dawn	7.96	1.91	98.4	170.0	77.5%

possible method for improving the CNT interconnections (Holesinger 2013). However, there was no significant difference in the coating resistivies between samples that either did or did not contain the added copper. Hence, Cu additions were not included in this first set of wires produced with the acid-based solutions.

A general trend in the data from Tables 1 and 2 is the general increase in the resistivity of the CNT coatings with thickness. The use of the acid-based solutions was inspired in part by the high conductivity results obtained from pure CNT fibers using cholorsulfonic acid. Indeed, the acid-based solutions used in this work were much more stable and did not readily separate when solution stirring was stopped. However, the general trend of lower CNT coating resistivities with thicker coatings was found with both processes, and the indications from structural analysis suggested a degradation of the coating uniformity with thickness, significant changes in the point-to-point thickness of the coatings, and the inclusion of large-scale porosity. The microstructural data of Figure 2 for the thick CNT coatings shows both of these aspects in the CNT coating. Conversely, the thin coatings (< 20 microns) tended to be much more uniform and quite dense. Hence, significant improvements in the coating process need to be made to further improve composite performance. This need inspired the use of conventional wire drawing to improve coating uniformity and density while removing porosity. These first results are quite promising, though it is noted (Fig. 4) that mechanical deformation itself can lead to other structural, current-limiting defects such as cracking. Work is in progress to refine these non-uniformities and produce thick (>200 μm), smooth, and aligned CNT coatings for strong, lightweight, and highly-conductive composite wires for use in advanced power applications.

Acknowledgements

Funding for the project is provided through the “Ultra-Deepwater and Unconventional Natural Gas and Other Petroleum Resources Research and Development Program” authorized by the Energy Policy Act of 2005. This program—funded from lease bonuses and royalties paid by industry to produce oil and gas on federal lands—is designed to assess and mitigate risk enhancing the environmental sustainability of oil and gas exploration and production activities. RPSEA is under contract with the U.S. Department of Energy’s National Energy Technology Laboratory to administer three areas of research. RPSEA is a 501(c) (3) nonprofit consortium with more than 180 members, including 24 of the nation's premier research universities, five national laboratories, other major research institutions, large and small energy producers and energy consumers. The mission of RPSEA, headquartered in Sugar Land, Texas, is to provide a stewardship role in ensuring the focused research, development and deployment of safe and environmentally responsible technology that can effectively deliver hydrocarbons from domestic resources to the citizens of the United States. Additional information can be found at www.rpsea.org.

The authors would also like to thank the Chevron Corporation and Susan Brockway and Don Hickmott (LANL) for their discussions and support of this project.

Table 2: List of whole wire and calculated CNT coating resistivities from wires produced with H_2SO_4 based solutions and wire drawn after coating, resistivity values for copper and aluminum in wire form (Weast 1983) and the wire used in this work prior to preparation and coating.

Wire	Wire Substrate	Dispersant	Wire Resistivity (μΩ-cm)	Substrate** Resistivity (μΩ-cm)	Calculated CNT Coating Resistivity (μΩ-cm)	Coating Thickness (μm)	CNT Coating: Percentage of Wire Cross Section
Cu (O_2 free)	---	---	1.68	---	---	---	---
Cu (annealed)	---	---	1.72	---	---	---	---
Cu (hard drawn)	---	---	1.77	---	---	---	---
26 AWG Cu Wire*	---	---	1.76	---	---	---	---
28 AWG Cu Wire*	---	---	1.78	---	---	---	---
Al	---	---	2.82	---	---	---	---
46_17	28 AWG Cu	H_2SO_4	2.12	1.82	7.9	16.8	18.5%
42_17	28 AWG Cu	H_2SO_4	2.22	1.83	15.1	18.3	20.0%
42_14	26 AWG Cu	H_2SO_4	2.17	1.80	27.8	20.8	17.9%
41_13	28 AWG Cu	H_2SO_4	2.44	1.86	27.6	23.1	25.1%
42_18	28 AWG Cu	H_2SO_4	2.36	1.81	60.6	23.2	24.3%
45_1	28 AWG Cu	H_2SO_4	2.45	1.87	25.2	25.0	25.6%
43_7	28 AWG Cu	H_2SO_4	2.43	1.85	20.0	25.3	26.1%
45_3	28 AWG Cu	H_2SO_4	2.45	1.82	46.1	25.5	26.5%
42_15	28 AWG Cu	H_2SO_4	2.33	1.84	9.3	25.9	27.6%
43_3	28 AWG Cu	H_2SO_4	2.52	1.87	46.1	26.8	27.0%
41_11A	28 AWG Cu	H_2SO_4	2.55	1.87	44.3	27.2	28.0%
46_9A	28 AWG Cu	H_2SO_4	2.48	1.79	41.7	28.3	28.8%
45_2	28 AWG Cu	H_2SO_4	2.62	1.89	26.6	30.3	29.9%
41_4A	26 AWG Cu	H_2SO_4	2.47	1.87	51.1	30.8	25.3%
41_12	28 AWG Cu	H_2SO_4	2.66	1.84	101.5	32.0	31.3%
43_5	28 AWG Cu	H_2SO_4	3.13	1.85	36.6	50.2	43.0%
44_11	28 AWG Cu	H_2SO_4	3.32	1.90	66.5	52.5	44.2%
44_1A	28 AWG Cu	H_2SO_4	3.40	1.87	133.3	54.0	45.6%
47_5	28 AWG Cu	H_2SO_4	3.57	1.87	70.6	61.0	48.9%
47_1	28 AWG Cu	H_2SO_4	3.58	1.84	165.5	61.8	49.2%

* Cu wire used for the wire former as measured directly off the roll, but before any preparation processes and coatings.

** Cu substrates / wire formers were cleaned and abraided prior to coating.

References

Behabtu, Natnael, Colin C. Young, Dmitri E. Tsentalovich et al. 2013. Strong, Light, Multifunctional Fibers of Carbon Nanotubes with Ultrahigh Conductivity *Science* **339** (6116): 182-186.

De Volder, Michael F. L., Sameh H. Tawfick, Ray H. Baughman et al. 2013. Carbon Nanotubes: Present and Future Commercial Applications *Science* **339** (6119): 535-539.

Holesinger, T. G. 2013. Unpublished Work

Iijima, Sumio. 1991. Helical microtubules of graphitic carbon *Nature* **354** (6348): 56-58.

Li, Chunyu, Tsu-Wei Chou. 2009. Electrical Conductivities of Composites with Aligned Carbon Nanotubes *Journal of Nanoscience and Nanotechnology* **9** (4): 2518-2524.

Li, Q. W, X. F Zhang, R. F DePaula et al. 2006. Sustained Growth of Ultralong Carbon Nanotube Arrays for Fiber Spinning *Advanced Materials* **18** (23): 3160-3163.

Liu, Kai, Yinghui Sun, Xiaoyang Lin et al. 2010. Scratch-Resistant, Highly Conductive, and High-Strength Carbon Nanotube-Based Composite Yarns (in *ACS Nano* **4** (10): 5827-5834.

Miao, Menghe. 2011. Electrical conductivity of pure carbon nanotube yarns *Carbon* **49** (12): 3755-3761.

Rastogi, Richa, Rahul Kaushal, S. K. Tripathi et al. 2008. Comparative study of carbon nanotube dispersion using surfactants *Journal of Colloid and Interface Science* **328** (2): 421-428.

Weast, Robert C., ed. 1983. *63rd Edition CRC Handbook of Chemistry and Physics*, CRC Press, Inc.

Zhao, Yao, Jinquan Wei, Robert Vajtai et al. 2011. Iodine doped carbon nanotube cables exceeding specific electrical conductivity of metals *Sci. Rep.* **1**.